Infrared Physics & Technology 80 (2017) 131–137

Contents lists available at ScienceDirect

Infrared Physics & Technology

journal homepage: www.elsevier.com/locate/infrared

Measurement of CO_2 concentration at high-temperature based on tunable diode laser absorption spectroscopy

Jiuying Chen [a], Chuanrong Li [a,*], Mei Zhou [a], Jianguo Liu [b], Ruifeng Kan [b], Zhenyu Xu [b]

[a] Key Laboratory of Quantitative Remote Sensing Information Technology, Academy of Opto-electronics, Chinese Academy of Sciences, Beijing 100094, China
[b] Key Lab in Environmental Optical Monitoring Techniques of Anhui Province, Anhui Institute of Optics and Fine Mechanics, Chinese Academy of Science, Hefei 230031, China

ARTICLE INFO

Article history:
Received 16 August 2016
Revised 27 November 2016
Accepted 28 November 2016
Available online 30 November 2016

Keywords:
Tunable diode laser absorption spectroscopy
CO_2 concentration
Line intensity
High-temperature spectrum

ABSTRACT

A diode laser sensor based on absorption spectroscopy has been developed for sensitive measurement of CO_2 concentration at high-temperature. Measurement of CO_2 can provide information about the extent of combustion and mix in a combustor that may be used to improve fuel efficiency. Most methods of *in-situ* combustion measurement of CO_2 use the spectroscopic parameters taken from database like HITEMP which is mainly derived from the theoretical calculation and remains a high degree of uncertainty in the spectroscopic parameters. A fiber-coupled diode laser system for measurement of CO_2 in combustion environment by use of the high-temperature spectroscopic parameters which are obtained by experiment was proposed. Survey spectra of the $R(50)$ line of CO_2 at 5007.787 cm^{-1} were recorded at high-temperature and various pressures to determine line intensities. The line intensities form the theoretical foundation for future applications of this diode laser sensor system. Survey spectra of four test gas mixtures containing 5.01%CO_2, 10.01%CO_2, 20.08%CO_2, and 49.82%CO_2 were measured to verify the accuracy of the diode laser sensor system. The measured results indicate that this sensor can measure CO_2 concentration with 2% uncertainty in high temperatures.

1. Introduction

The availability of new lasers in the near and mid-infrared spectral region has led to the development of sensors for gas measurements that are now applied extensively in a variety of environments. Based on tunable diode laser absorption spectroscopy (TDLAS) molecules like O_2, CH_4, H_2O, CO, CO_2, NH_3, HCl, and HF can be detected *in-situ* with high selectivity and sensitivity in continuous, real-time operation [1–3]. TDLAS is a non-intrusive, high sensitivity, interference immunity measurement technique for determining temperature, species concentration, velocity, pressure and other gas-dynamic properties in various gaseous environments [4–6].

In the hydrocarbon fuel combustion, CO_2, CO, and H_2O are the main products of combustion. Their concentrations can both represent combustion position and play a vital role in evaluating combustion parameters such as combustion efficiency, burning degree, and heat release [7,8]. CO_2 and CO are called the key indicators of combustion efficiency. Accurate measurement of CO_2 in the combustion flow field is very important for energy conservation and emission reduction in the industrial combustion process and engine combustion state diagnosis.

Previous approaches to *in-situ* measurements of post-flame CO_2 were conducted around 1.57 μm by using the transitions of $3\nu_1+\nu_3$ band [9] or $2\nu_1+2\nu_2^0+\nu_3$ band [3]. However, the absorption bands of CO_2 near 2 μm are approximately 2 orders of magnitude larger than at about 1.57 μm. The strong CO_2 transitions near 2.0 μm have already been adopted in combustion measurement applications using absorption spectroscopy and extractive sampling techniques [10]. The problem with CO_2 measurement in combustion applications is the line intensities at high-temperature taken from the HITRAN/HITEMP database have uncertainties of 10% or higher [11]. In this paper, the line intensities of the $R(50)$ line of CO_2 at high-temperature up to 1873 K were first measured by an experiment using the experimental setup which was designed to measure spectroscopic parameters at high-temperature. The measurement of line intensities with accuracy less than 1.5% can improve the measurement accuracy of CO_2 concentration at high-temperature. The results of this study make the CO_2 probing technique a promising application for combustion diagnosis.

* Corresponding author.
E-mail addresses: jychen@aoe.ac.cn (J. Chen), crli@aoe.ac.cn (C. Li).

http://dx.doi.org/10.1016/j.infrared.2016.11.016
1350-4495/

2. Theory

2.1. Absorption spectroscopy

The relationship between the transmitted and incident intensity of radiation that has passed through a gas medium of path length, L, is described by the Beer-Lambert law:

$$I/I_0 = \exp(-k_v L) \tag{1}$$

where I_0 is the incident intensity, I is the transmitted intensity, for a single transition i, k_v [cm^{-1}] is:

$$k_v = P x_{abs} S_i(T) \phi_v \tag{2}$$

where P is the total static pressure [atm], x_{abs} is the mole fraction of the absorbing species, $S_i(T)$ is the transition line intensity [cm^{-2}·atm^{-1}], and ϕ_v is the normalization line-shape function [cm], namely, $\int \phi_v dv = 1$. From Eqs. (1) and (2), we can calculate integrated absorbance as follows:

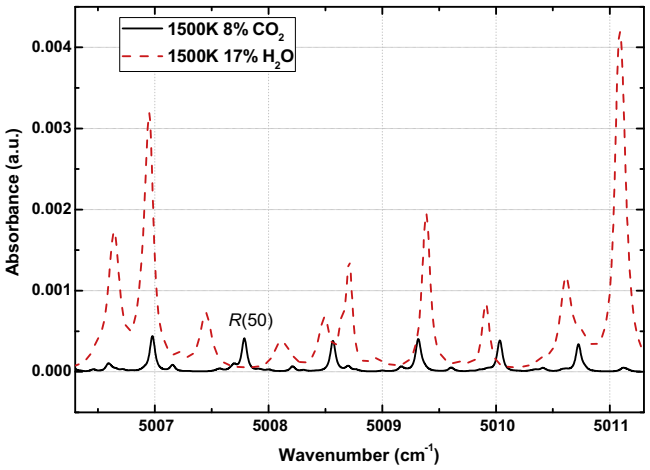

Fig. 1. Calculated spectra of 8% CO_2 and 17% H_2O near 5007.787 cm^{-1} at combustion conditions (L = 1 cm, P = 1 atm, T = 1500 K). The $R(50)$ transitions of the $\nu_1 + 2\nu_2^0 + \nu_3$ band at 5007.787 cm^{-1} is partially isolated from high-temperature water interference.

$$A_i = \int \ln(I_0/I)\, dv = P x_{abs} S_i(T) L \tag{3}$$

The mole fraction of the absorbing species can be given by:

$$x_{abs} = A_i / P S_i(T) L \tag{4}$$

The temperature dependent line intensity can be calculated as follows:

$$S(T) = S(T_0)\frac{Q(T_0)}{Q(T)}\left(\frac{T_0}{T}\right)\exp\left[-\frac{hcE''}{k_B}\left(\frac{1}{T}-\frac{1}{T_0}\right)\right] \times \left[1-\exp\left(\frac{-hc\nu_0}{k_B T}\right)\right]\left[1-\exp\left(\frac{-hc\nu_0}{k_B T_0}\right)\right]^1 \tag{5}$$

where h is Plank's constant, c is the speed of light, k_B is Boltzmann's constant, and $Q(T)$ is the partition function for the absorbing species [12].

2.2. Propagation of error for mole fraction

Propagation of error (or propagation of uncertainty) is defined as the effects on a function by a variable's uncertainty. It is a calculus derived statistical calculation designed to combine uncertainties from multiple variables, in order to provide an accurate measurement of uncertainty. Typically, the error is given by the standard deviation of a measurement. Anytime a calculation requires more than one variable to solve, propagation of error is necessary to properly determine the uncertainty.

The propagation of error formula for $x = f(u, v, \ldots)$ a function of one or more variables with measurements, $u, v, \ldots$ are independent, gives the following estimate of the standard deviation of x:

$$\sigma_x \approx \sqrt{\sigma_u^2(\partial x/\partial u)^2 + \sigma_v^2(\partial x/\partial v)^2 + \cdots} \tag{6}$$

where σ_u is the standard deviation of u measurements, σ_v is the standard deviation of v measurements, $\partial x/\partial u$ is the partial derivative of the function x with respect to u, etc.

The mole fraction Eq. (4) can be rewritten as:

$$\ln x_{abc} = \ln A_i - \ln P - \ln L - \ln S_i \tag{7}$$

From Eq. (7),

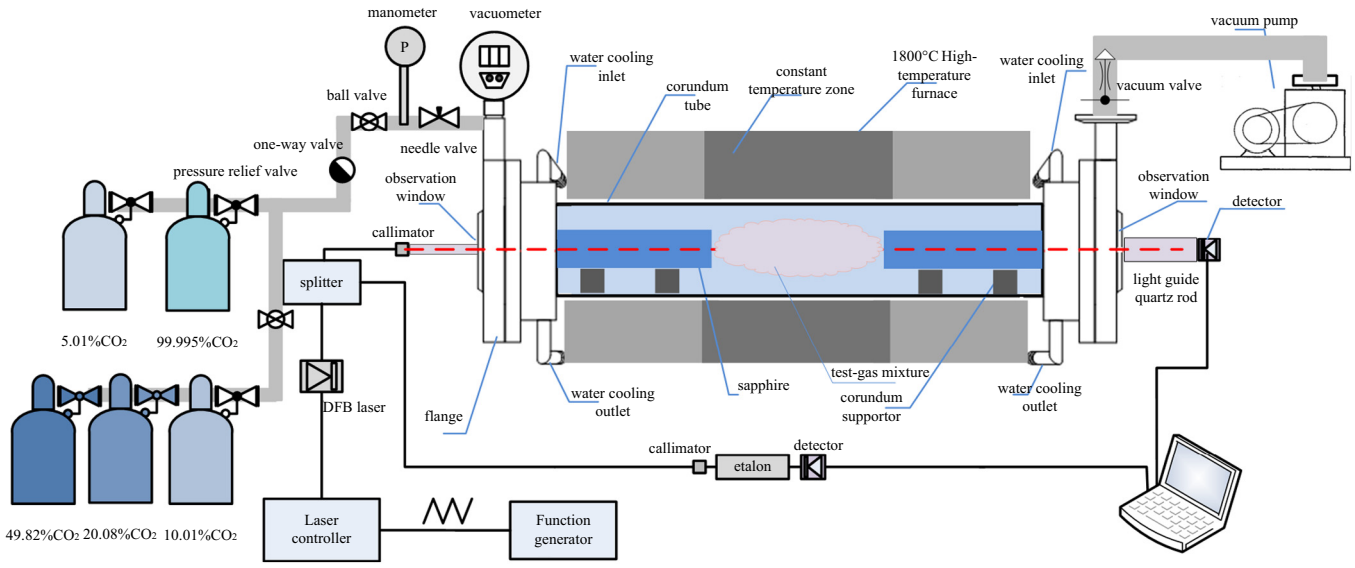

Fig. 2. Schematic diagram of experimental measurement equipment.

$$\partial \ln x_{abc}/\partial A_i = 1/A_i$$
$$\partial \ln x_{abc}/\partial P = -1/P$$
$$\partial \ln x_{abc}/\partial L = -1/L$$
$$\partial \ln x_{abc}/\partial S_i = -1/S_i$$

In combination with Eq. (6), the relative standard deviation of mole fraction is:

$$\sigma_x/x = \sqrt{(\partial \ln x/\partial A_i)^2\sigma_{A_i}^2 + (\partial \ln x/\partial P)^2\sigma_P^2 + (\partial \ln x/\partial L)^2\sigma_L^2 + (\partial \ln x/\partial S_i)^2\sigma_{S_i}^2}$$
$$= \sqrt{(\sigma_{A_i}/A_i)^2 + (\sigma_P/P)^2 + (\sigma_L/L)^2 + (\sigma_{S_i}/S_i)^2} \quad (8)$$

3. Selection of line

The selection of optimum absorption transitions is the first and foremost step in designing a TDL sensor. Simulated spectra based on the HITRAN database are computed for combustion conditions (T = 1000–2500 K, P = 1 atm) to find suitable transitions. The HITEMP database is used to identify additional high-temperature transitions that are not listed in HITRAN. A systematic line-selection procedure has been developed in the literature [13,14]. These same design rules are used here to select the optimum 2.0 μm CO_2 line for measurement of CO_2 in a combustion environment.

The first criterion used limits the spectral region for selection of candidate CO_2 transitions. The band strength of the CO_2 $\nu_1 + 2\nu_2^0 + \nu_3$ band near 2.0 μm is approximately a factor of 73 larger than the $2\nu_1 + 2\nu_2^0 + \nu_3$ band near 1.58 μm. As a result, laser absorption measurements near 2.0 μm offer the potential for significantly increased detection sensitivity for species concentration measurements relative to shorter-wavelength diode lasers.

The second criterion is to ensure that the absorption strength of candidate transitions is large enough to guarantee a high signal-to-noise (SNR) ratio but small enough to avoid optically thick measurements over the expected conditions typical of hydrocarbon combustion products (T = 1000–2500 K, P = 1 atm, L = 10 cm, x_{CO_2} = 0.08–0.1).

The third criterion is to choose transitions that are free from the interference of other combustion species such as H_2O, CO, NO, CH_4. Calculated absorption spectra of high-temperature H_2O and CO_2 were used to find candidate transitions for CO_2 detection as shown in Fig. 1.

The fourth criterion is to select transitions that have minimal interference from ambient CO_2 and cold boundary layers. If a transition has a strong absorption coefficient at room temperature, the measurement accuracy is compromised if the region outside the target measurement is not purged completely of ambient CO_2. Use of transitions with relatively large lower state energy (E'') ensures that the absorption at room temperature is much smaller than that at combustion temperatures. Here we select transitions having a minimum E'' of 900 cm^{-1}.

Applying the aforementioned criteria, the $R(50)$ transition at 1.997 μm ($\nu_1 + 2\nu_2^0 + \nu_3$ band) was selected based on its line intensity, lower state energy (994.19 cm^{-1}) and isolation from interfering high-temperature water absorption in this paper.

4. Experimental details

Fig. 2 shows a schematic of the experimental setup consisting of the diode-laser system and the high-temperature static cell that was used to measure 5.01%CO_2, 10.01%CO_2, 20.08%CO_2, 49.82% CO_2 and 99.995%CO_2 absorption spectra. DFB laser made by Nanoplus whose center wavenumber is near 5007.8 cm^{-1} works in current scanning mode. The wavenumber scanning range is from 5005.6 cm^{-1} to 5008.8 cm^{-1}. The laser radiation beam is divided into 2 beams by a fiber splitter. The main beam which is 90% enters the corundum tube by a fiber collimator and the light guide quartz rod, then goes through sapphire round rod made by Constone Sapphire Technology Co., Ltd., at last, arrives at the constant temperature zone containing test gas mixture. The laser beam with the CO_2 absorption spectrum information passing through the sapphire round rod, light guide quartz rod on the right, arrives at a photoelectric detector (Thorlabs, PDA10D-EC), whose output signal is acquired by a data acquisition card (NI, PCI 5105). The signals were then digitized (12-bit A/D converter) and transferred via PCI to a personal computer for analysis. The other beam which is 10% passes through the etalon (Shanghai Institute of Optics and Fine Mechanics, 10 cm in length) which is used to measure the laser wavelength variations.

In Fig. 2 and 1800 °C high-temperature furnace (MTI, GSL-1800X-III) is an 1800 °C three temperature zone tube furnace

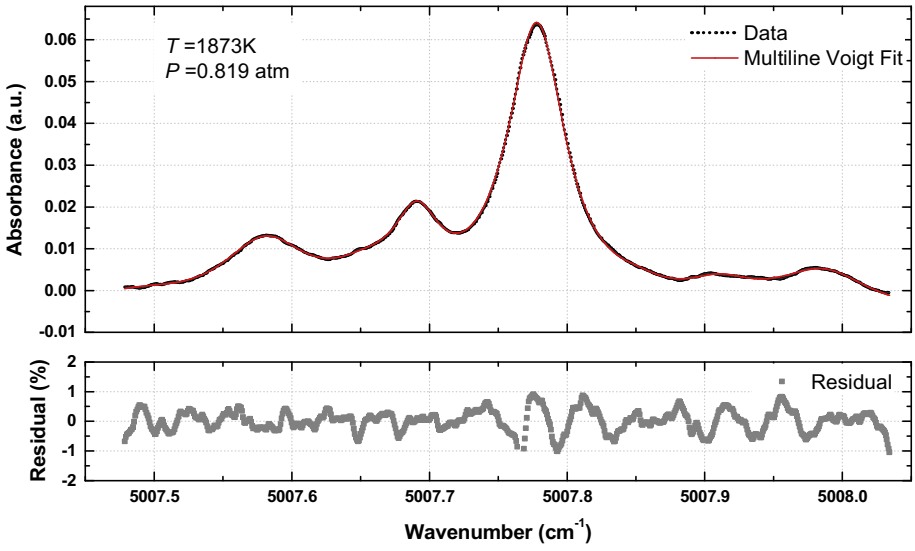

Fig. 3. Measured spectral absorbance of CO_2 and multiline Voigt fit at 1873 K. The residual represents the normalized difference between the data and the multi-line combined best-fit Voigt profile.

(maximum temperature up to 1800 °C), using imported Kathal Super-1900 °C Si-Mo bar as a heating element, equipped with a diameter 60 mm stainless steel water cooled sealing flange, sealed by high-temperature resistant silica gel O-type ring. The temperature control system of the high-temperature furnace includes 3 digital temperature controllers, using PID method to adjust the temperature, and the temperature control accuracy is ±1 K. The temperatures of three zones were measured with 3 type-B thermocouples (verified accuracy < 0.5 K for 873–1973 K). The length of the constant temperature zone is 32.35 cm, and the measurement uncertainty is less than 0.02%. The one-way valve is used to prevent heat reflux, and the vacuum degree of the cell reaches a few mTorr with the use of a vacuum pump (KYKY Technology Co., Ltd., RVD-4). Two light guide quartz rods are used to isolate thermal radiation and the air in the light path, and an etalon is used to measure the laser wavelength variations.

A vacuum gauge (INSTRUTECH, Stinger CVM211) mounted on the sealing flange as shown in Fig. 2 was used to monitor the cell pressure. The measurement range of the vacuum gauge is 0.1 mTorr–1000 Torr, and the measurement accuracy is ±1%. Gas with purities of 99.995% CO_2 was used for line intensity measurements. The cell was repeatedly flushed with the test gas and evacuated to less than 5 mTorr using the vacuum pump before each measurement to ensure a high gas purity inside the cell. The test gas needs to be heated for at least 1 h at the measurement temperature in order to achieve steady and uniform temperature inside the cell. Survey spectra of the CO_2 $R(50)$ line of the test gas were measured at high temperatures between 1273 K and 1873 K. The data obtained at each time was the average value in 64 times to reduce the random errors.

5. Result

5.1. Line intensity

Survey spectra of the CO_2 $R(50)$ line of pure CO_2 gas at temperatures between 1273 K and 1873 K were measured by experiments. There were 6–8 different pressures at each temperature.

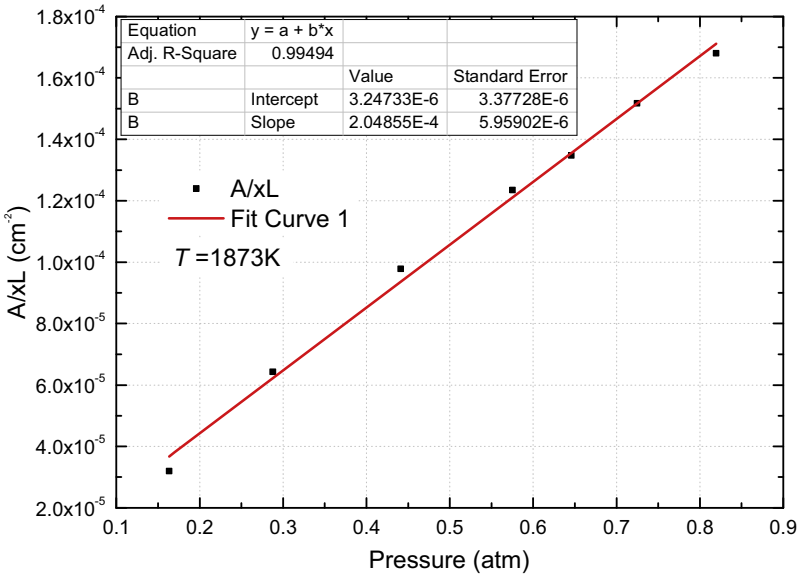

Fig. 4. The ratio of measured integral absorbance to product of mole fraction and path (A/xL) as a function of pressure at 1873 K.

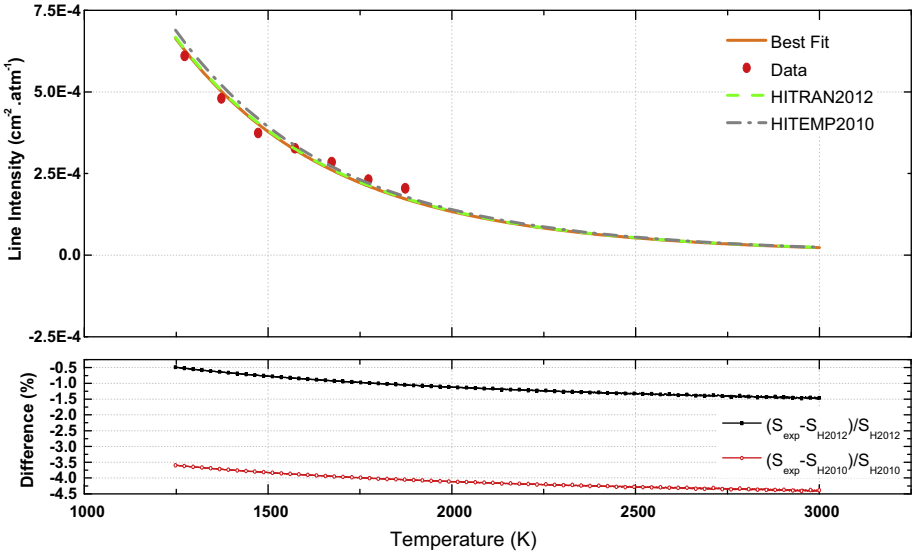

Fig. 5. Comparison of intensities (HITRAN2012 database and HITEMP2010 database) and measured intensities of CO_2 $R(50)$ line.

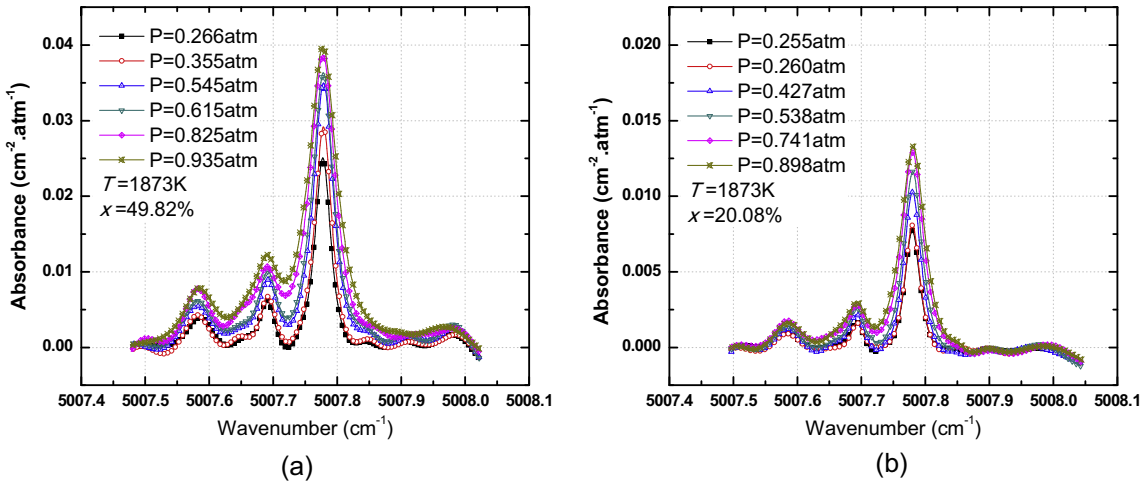

Fig. 6. The CO_2 absorbance curves of 49.82% CO_2 and 20.08%CO_2 under different pressures at 1873 K.

First, convert the survey spectra in the time domain to absorbance curves in the frequency domain [15], then, make multi-line combined nonlinear least squares fitting on the absorbance curves [16], the measured spectral absorbance of CO_2 and multiline Voigt fit at temperatures between 1273 K and 1873 K can be obtained. With the increasing of temperature in the 1273–1873 K temperature range, the peaks of CO_2 absorbance curve gradually decrease, the interference absorptions on both sides of the main peak relatively enhance, and high-temperature survey spectra are more complex. Fig. 3 is the measured spectral absorbance of CO_2 and multiline Voigt fit at 1873 K. The residual is calculated from the normalized difference between the data and the best-fit multiline combined Voigt profile. The Voigt fit has a maximum deviation of 1% from the measured data. According to Eq. (6), the total uncertainty for the individual line intensity measurements was estimated to be approximately 1.5%, resulting from measurement uncertainties of 1% in the total pressure, 1% in the area under each Voigt profile, 0.01% in the concentration of CO_2, and 0.02% in the path length.

The ratios of measured integral absorbance and product of mole fraction and path (A/xL) of several different presses at 1873 K are shown in Fig. 4. The best-fit line slope in Fig. 4 is the line intensity at 1873 K according to Eq. (4).

The measured $R(50)$ line intensities at temperatures between 1273 K and 1873 K are shown in Fig. 5. The intensities will be used to calculate test gas concentrations. In the upper part of Fig. 5, the green[1] dashed line represents the fitting intensity curve according to HITRAN2012 database, the gray dotted line represents the fitting intensity curve according to HITEMP2010 database, the red dots represent the measured values from the experiment, and the light red curve represents the fitting intensity curve according to experimental values. As can be seen from this figure, the experimental values are very close to the literature values. The relative differences between the measured line intensities and the literature values as a function of temperature are shown in the lower part of Fig. 5. The measured line intensities are more close to HITRAN2012 than HITEMP2010, which are approximately 1.5% lower than the values listed in HITRAN2012, and 4.5% lower than the values listed in HITEMP2010. Because the total experimental uncertainty is 1.5%, compared with 2% for the value in HITRAN2012 and 20% for the

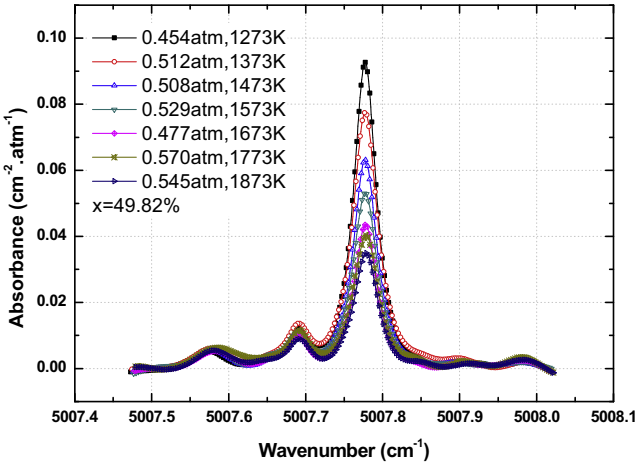

Fig. 7. Absorbance curves of 49.82%CO_2 at different temperatures.

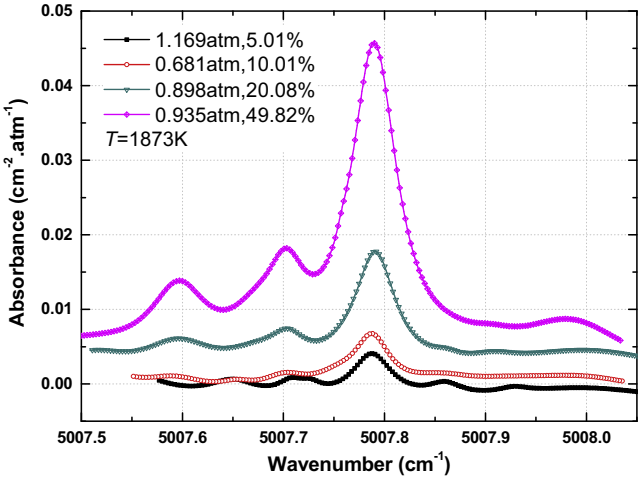

Fig. 8. Absorbance curves of 5.01%CO_2, 10.01%CO_2, 20.08%CO_2, 49.82%CO_2 at 1873 K (there is a small vertical offset at each curve).

[1] For interpretation of color in Figs. 5 and 9, the reader is referred to the web version of this article.

value in HITEMP2010, we consider those measured line intensities to be better than the published values.

5.2. Concentration

Survey absorption spectra of 5.01%CO_2, 10.01%CO_2, 20.08%CO_2, 49.82%CO_2 and 99.995%CO_2 at different temperatures and pressures were measured using high-temperature static cell experimental measurement equipment. For example, Fig. 6 shows the CO_2 absorbance curves of 49.82%CO_2 and 20.08%CO_2 under different pressures at 1873 K. It can be seen from this figure that with the increasing of total static cell pressure, the spectral lines gradually expand, adjacent transitions overlap. The greater the pressure is, the more serious the overlaps are, and the more serious the interferences between the transitions are.

The absorbance curves at different temperatures were gotten by use of the multi-line combined nonlinear least squares method. For example, Fig. 7 shows the absorbance curves of 49.82%CO_2 at different temperatures. The areas underneath individual absorbance of $R(50)$ at different temperatures were obtained. From the figure, in the temperature range from 1273 K to 1873 K, with the increasing of temperature, the peak of absorbance curve at 5007.787 cm^{-1} gradually reduces, the integral absorbance decreases gradually, which is agreed with the change trend of the intensity at 5007.787 cm^{-1} with the change of temperature.

The absorbance curves of CO_2 in different test gas mixtures at the same temperature were present in one diagram, as shown in Fig. 8. At the same temperature (taking T = 1873 K as an example), the line intensity of $R(50)$ line is constant. With the increasing of the CO_2 concentration of test gas mixture, the peak of the absorbance curve increases gradually, and the integral absorbance was proportional to the concentration. For the convenience of observation and comparison, all vertical coordinates of the absorbance curve of different CO_2 concentration increase a small offset.

The measured concentrations of CO_2 in test gas mixtures at temperatures from 1273 K to 1873 K are shown in Fig. 9. The red solid lines represent the nominal concentrations of test gas mixture x_{nc} , the pink dotted lines respectively represent 5% more (or less) than the nominal concentrations of test gas mixture, namely x_{nc} ± 5%, the black dots indicate the measured concentrations in the figure. As can be seen from the figure, the black dots (measured concentrations) are all between the two pink dotted lines (x_{nc} ± 5%), that is, the differences between measured concentrations and nominal concentrations of test gas mixture are less than 5%. The feasibility of CO_2 concentration measurement method was verified.

The measured concentrations and measurement error at temperatures from 1273 K to 1873 K are listed in Table 1. The mean is the average value of the measured concentrations of one test gas mixture at different temperatures, the standard deviation is the square root of the variance of the measured concentration, and the relative standard deviation is the ratio of the standard deviation and the mean. The relative deviation is the ratio of the difference between the measured mean and the nominal value of

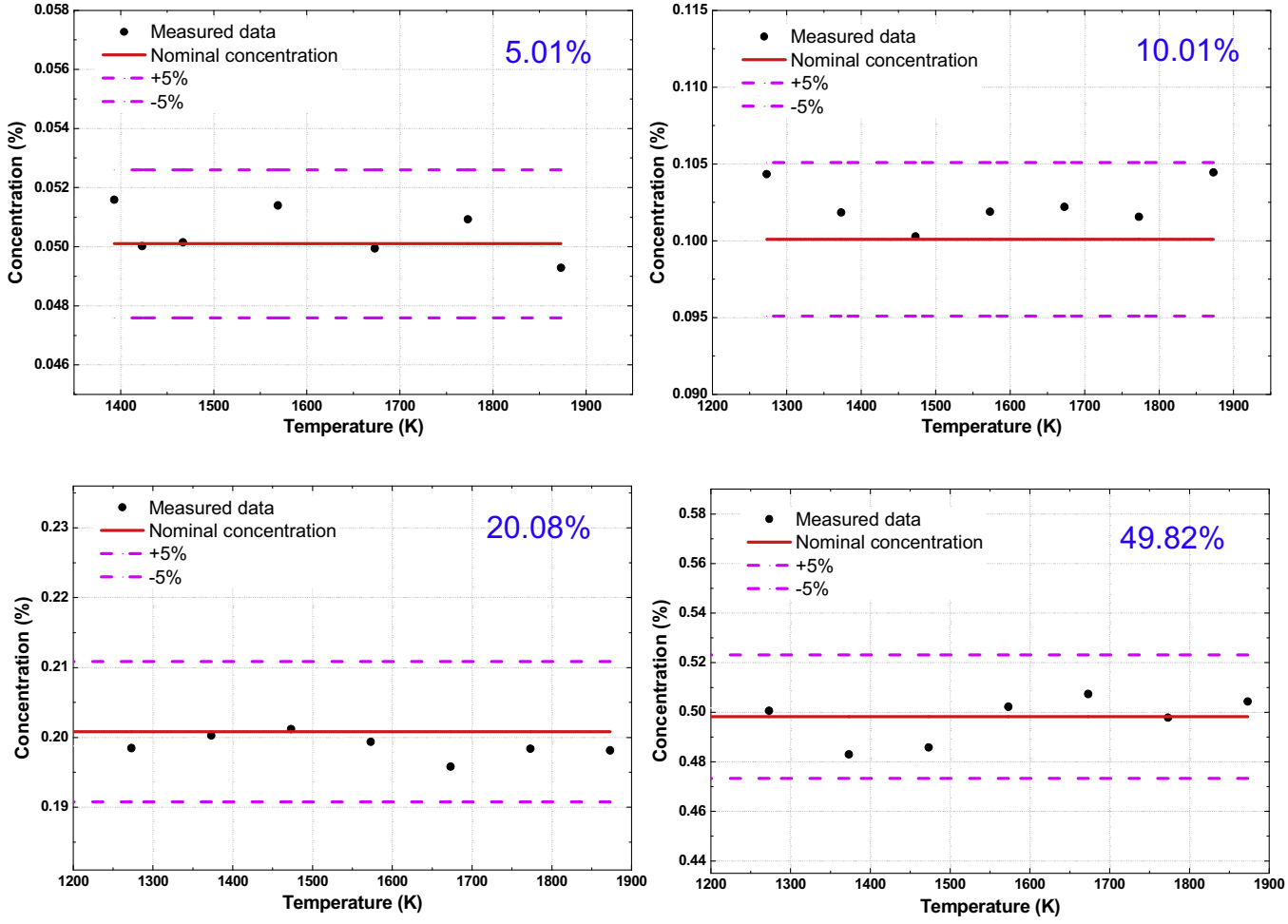

Fig. 9. Measured concentrations at temperatures from 1273 K to 1873 K.

Table 1
Measured concentrations and measurement error.

	T (K)	x (%)	T (K)	x (%)	T (K)	x (%)	T (K)	x (%)
Measured concentrations at different temperatures	1393	5.159	1273	10.434	1273	19.845	1273	50.055
	1423	5.002	1373	10.185	1373	20.026	1373	48.295
	1467	5.015	1473	10.028	1473	20.118	1473	48.585
	1569	5.140	1573	10.189	1573	19.936	1573	50.220
	1673	4.995	1673	10.221	1673	19.581	1673	50.732
	1773	5.093	1773	10.155	1773	19.837	1773	49.779
	1873	4.929	1873	10.445	1873	19.813	1873	50.435
Nominal concentrations	–	5.01	–	10.01	–	20.08	–	49.82
Measured mean	–	5.047	–	10.237	–	19.926	–	49.955
Standard deviation	8.46×10^{-4}		1.51×10^{-3}		2.06×10^{-3}		1.08×10^{-2}	
Relative standard deviation	1.677%		1.480%		0.867%		1.876%	
Relative deviation	0.739%		2.268%		1.001%		0.183%	

the test gas mixture and the nominal value. It can be seen from the table that in the temperature range of 1273–1873 K for CO_2 concentration measurement of test gas mixtures with 5–50% CO_2, the relative deviation is less than 3%, and the relative standard deviation is less than 2%, which indicate that the accuracy and precision of the CO_2 concentration measurement method are relatively ideal.

According to Eq. (8), the estimated experimental uncertainty of CO_2 concentrations inferred from measurements (<2%) was limited by the uncertainty of the pressure measurement (<1%), the uncertainty of the path length (<0.02%), the uncertainty of line intensity (<1.41%) and the uncertainty in the area underneath individual absorbance (<1%). It agrees with the relative standard deviation in Table 1 very well.

6. Conclusion

A CO_2 sensor for combustion environments that used diode-laser absorption techniques has been developed and demonstrated. Calculated high-temperature absorption spectra of CO_2 and H_2O were overlaid to find suitable transitions for *in situ* monitoring, yielding one candidate: the $R(50)$ transition at 5007.787 cm^{-1}. The $R(50)$ transition was selected for the CO_2 diagnostic on the basis of its line strength and its isolation from water interference at combustion temperatures. Line intensities for this transition were measured and compared with the literature values, resulting in improved line intensities with an uncertainty of 1.5%. The system evaluation was done in a high-temperature static cell with test gas of various CO_2 concentrations. The measured results indicate that this sensor can measure CO_2 gas concentration with better than 2% uncertainty. It was found that the CO_2 concentration measurement method could be performed in engine combustion diagnostics.

Acknowledgments

This work is supported by the research project-Research on laser active remote sensing method for column concentration of tropospheric CO_2 founded by Innovation Program of Academy of Opto-Electronics (AOE), Chinese Academy of Science (CAS) [grant numbers Y40B07A14Y].

References

[1] M. Lackner, Tunable diode laser absorption spectroscopy (TDLAS) in the process industries–a review, Rev. Chem. Eng. 23 (2) (2007) 65–147.
[2] D.M. Sonnenfroh, M.G. Allen, Diode laser sensors for combustor and aeroengine emissions testing: applications to CO, CO2, OH, and NO, AIAA, 1996, 96–2226.
[3] R.M. Mihalcea, D.S. Baer, R.K. Hanson, Diode laser sensor for measurements of CO, CO_2, and CH_4 in combustion flows, Appl. Opt. 36 (33) (1997) 8745–8752.
[4] J.T.C. Liu, J.B. Jeffries, R.K. Hanson, Wavelength modulation absorption spectroscopy with 2f detection using multiplexed diode lasers for rapid temperature measurements in gaseous flows, Appl. Phys. B 78 (2004) 503–511.
[5] P. Werle, F. Slemr, K. Maurer, R. Kormann, R. Mücke, B. Jänker, Near-and mid-infrared laser-optical sensors for gas analysis, Opt. Laser Eng. 37 (2) (2002) 101–114.
[6] T.D. Cai, G.S. Wang, Z.S. Cao, W.J. Zhang, X.M. Gao, Sensor for headspace pressure and H_2O concentration measurements in closed vials by tunable diode laser absorption spectroscopy, Opt. Laser Eng. 58 (2014) 48–53.
[7] M.P. Arroyo, R.K. Hanson, Absorption measurements of water vapor concentration, temperature, and line-shape parameters using a tunable InGaAsP diode laser, Appl. Opt. 32 (30) (1993) 6104–6116.
[8] A. Farooq, H. Li, J.B. Jeffries, R.K. Hanson, Measurements of CO_2 and H_2O near 2.7 μm using tunable diode laser absorption, in: 43rd AIAA/ASME/SAE/ASEE Joint Propulsion Conference & Exhibit. Cincinnati, USA: AIAA, 2007 (5015/1-5015/9).
[9] D.M. Sonnenfroh, M.G. Allen, Observation of CO and CO_2 absorption near 1.57 μm with an external-cavity diode laser, Appl. Opt. 36 (15) (1997) 3298–3300.
[10] R.M. Mihalcea, M.E. Webber, D.S. Baer, R.K. Hanson, G.S. Feller, W.B. Chapman, Diode-laser absorption measurements of CO_2, H_2O, N_2O, and NH3 near 2.0 μm, Appl. Phys. B 67 (3) (1998) 283–288.
[11] W.J. Phillips, D.H. Plemmons, N.A. Galyen, HITRAN/HITEMP spectral databases and uncertainty propagation by means of Monte Carlo simulation with application to tunable diode laser absorption diagnostics, No. AEDC-TR-11-T-2, Office of the deputy undersecretary of defense (science and technology) Washington DC joint technology office on hypersonic, 2011, pp. 15–17.
[12] V. Nagali, S.I. Chou, D.S. Baer, R.K. Hanson, J. Segall, Tunable diode-laser absorption measurements of methane at elevated temperature, Appl. Opt. 21 (1996) 4026–4031.
[13] X. Zhou, X. Liu, J.B. Jeffries, R.K. Hanson, Development of a sensor or temperature and water concentration in combustion gasses using a single tunable diode laser, Meas. Sci. Technol. 14 (2003) 1459–1468.
[14] A. Farooq, J.B. Jeffries, R.K. Hanson, In situ combustion measurements of H_2O and temperature near 2.5 μm using tunable diode laser absorption, Meas. Sci. Technol. 19 (2008) 075604.
[15] J.Y. Chen, J.G. Liu, Y.B. He, L. Wang, Q. Gang, Z.Y. Xu, L. Yao, S. Yuan, J. Ruan, J.F. He, Y.H. Dai, R.F. Kan, Study of CO_2 spectroscopic parameters at high temperature near 2.0 μm, Phys. Sin-Chinese Ed. 22 (2013) 212–218.
[16] J.Y. Chen, J.G. Liu, Y.B. He, Z.Y. Xu, H. Li, L. Yao, S. Yuan, J. Ruan, J.F. He, R.F. Khan, Temperature measurement of CO_2 by use of a distributed-feedback diode laser sensor near 2.0 μm, Chinese J Lasers 11 (2012) 117–121.

Jiuying Chen (1982–), female, doctor. Her current research interests include tunable diode laser absorption spectroscopy, environmental optical monitoring technique.